

Predicting Wave Run-Up using Full ALE Finite Element Approach considering Moving Boundary

Shahin Zohouri¹, Moharram D. Pirooz², and Asad Esmaily³

Abstract: A numerical scheme is developed to predict the wave run-up of an unsteady, incompressible viscous flow with free surface by the author¹. The method involves a two dimensional finite element with moving boundaries. The governing equations were the Navier-Stokes equations for conservation of momentum and mass for Newtonian fluids, continuity equation, and full nonlinear kinematic free-surface equation. A mapping algorithm was developed to solve highly deformed free surface problems, common in wave propagation. This algorithm transforms the run up model from the physical domain to a computational domain. A new Arbitrary Lagrangian-Eulerian (ALE) finite element modeling technique was used to model the fluid flow and predict the wave modification. Oscillation of the surface profile near the vertical wall was corrected by using a numerical procedure in the mapping function, and also by employing moving boundary technique at the wall point where run up happens. These oscillations are associated with mapping process at the boundaries when a full ALE finite element approach is used in both coordinate directions.

keyword: Wave run-up, finite element, free surface, conformal mapping, ALE, moving boundary.

1 Introduction

The numerical solution of gravity free surface waves has been developed in previous works using Lagrangian and Eulerian fluid description. Arbitrary Lagrangian-

Eulerian formulation, as a method developed in recent years, employs three phases to trace fluid motion. In the first phase, the free surface is upgraded by Lagrangian description. In the second phase called "rezoning phase", the rezoned velocities and the new grids are specified such that the distortion in fluid domain is reduced. In the last phase, the convective terms reserved from the first phase are calculated. To eliminate the rezoning phase and reduce the computational time, a new method, as discussed in this paper, is developed. This method is based on a new Arbitrary Lagrangian-Eulerian description of the fluid domain in which, the nodal points are displaced independent of the fluid motion, satisfying a set of particular equations (transformation functions), with a fixed computational grid. Nodal displacements in both coordinate directions result in a full Arbitrary Eulerian-Lagrangian approach.

The method discussed here, as a modified formulation of the Arbitrary Lagrangian-Eulerian description, in which rezoning is determined in advance, leads to a better treatment of fluid interfaces with a lower computational time.

For the present study, the flow is assumed to be viscous and incompressible. No artificial viscosity is introduced in the kinematic free surface equations to damp out the free surface oscillations in the region. The equations of conservation of momentum and mass for incompressible Newtonian fluids given by Navier-Stokes, and continuity equation along with full nonlinear kinematic free surface equation, are adopted as the governing equations. A particular mapping technique is used to transform the fluid region and its boundaries into a regular geometry for a convenient treatment of the moving free surface and irregular bottom topography. This leads to transformation of the governing equations and the boundary conditions into more complicated equations. However, the transformed equations can be effectively handled by a proper analytical and numerical procedure. In the full Arbitrary Lagrangian-Eulerian approach, mesh grids move in both

¹ PHD. Graduate, Department of Civil Engineering, University of Tehran, Tehran, Iran, Tel:+98-261-350 2496, E-mail: szohouri@ut.ac.ir

² Assistant Professor, Department of Civil Engineering, University of Tehran, Tehran, Iran, Tel: +98-21-611 3294, E-mail: mdolat@ut.ac.ir

³ Assistant Professor, Department of Civil Engineering, Kansas State University, Fiedler Hall 2118, Manhattan, KS 66506-2905, Tel: (785)- 532 6063, Fax: (785)- 532 7717, E-mail: asad@ksu.edu

directions of the domain, leading to oscillations at the run up boundary. These oscillations are associated with the mapping process. This paper addresses this problem by using two different techniques. Validity and efficiency of the proposed algorithms are examined for both cases by comparing the results with the available numerical approaches to predict wave run-up over vertical wall.

The developed techniques could easily be extended to analyze many other free surfaces problems such as run-up over sloping beaches.

2 The Field of Related Research Works

Different algorithms have been employed to solve free surface problems. A higher order theory is required to address the nonlinearity effects of extra large free surface displacements. Navier-Stokes equations are suitable for a variety of problems in fluid mechanics including extra large free surface displacements, and have been used in different methods by researchers in this field.

Wellford and Ganaba [1981] analyzed free surface problems involving extra large free surface motions using finite element techniques. They employed a spatially fixed Eulerian mesh in conjunction with a moving Lagrangian free surface line. Fenton and Rienecker [1982] have developed a Fourier method to address the interaction of solitary waves with an impermeable wall, whereas Kim et al. [1983] used the Boundary Integral Equation Method (BIEM) for the same problem. The asymptote for the maximum run-up of solitary waves on plane beaches has been derived by Synolakis [1987] using an approximate theory, supported by a series of laboratory experiments by Hall and Watts [1953], Camfield and Street [1969] and Kishi and Saeki [1966].

Zelt [1986] parameterized the wave breaking with an artificial viscosity term in the momentum equation to damp out the oscillation of free surface right behind the bore. Furthermore, Zelt [1991] investigated the run-up of non-breaking and breaking solitary waves on plane impermeable beaches by using his Boussinesq wave model and a Lagrangian finite element method. Ramaswamy and Kawahara [1987] adopted an Arbitrary Lagrangian-Eulerian description to solve free surface flow involving large free surface motion using finite element techniques. Grilli and Svendsen [1989] used a BIEM to solve fully nonlinear solitary waves interacting with both plane, gentle, and steep slopes. Solitary wave generation, propaga-

tion and Run-up are well described and forces for a vertical wall case are also calculated in their method. Hayashi et al. [1991] applied a finite element analysis on the Lagrangian description, combined with a fractional step method to solve unsteady incompressible viscous fluid flow governed by Navier-Stokes equations. Although their formulation was based on viscous fluid, the viscosity was considered equal to zero in application to find the wave run-up in a tank. Liu et al. [1994] employed the staggered leap-frog method in solving the shallow water equations and studied the large-scale tsunami propagation in ocean and inundation in coastal areas. Using the same model, they also simulated the solitary wave run-up on a circular island. Titov and Synolakis [1995] developed a finite difference model using Godunov method (second-order approximation in space and first-order in time) to simulate the same problem. No eddy viscosity was considered in their model and the energy decay due to turbulence was handled by numerical dissipation.

Zelt [1991], and Titov and Synolakis [1995] have shown that the depth-averaged equations models cannot always describe the evolution of breaking solitary waves as well as they can calculate the maximum Run-up.

Dolatshahi and Wellford [1995] analyzed free surface profile with a two dimensional Arbitrary Lagrangian-Eulerian finite element method to predict wave breaking. They computed the wave run-up over vertical wall by employing Eulerian description in wave propagation direction and Lagrangian description in vertical direction. Oscillation of the free surface on the vertical wall due to mesh movement in the x direction was a deficiency in this method. Detailed characteristics of solitary waves shoaling over plane slopes and those of solitary wave breakers, like jet shape and wave height variation, were studied subsequently by Grilli et al. [1997]. Titov and Synolakis [1998] have extended their inviscid solution to two dimensional topographies and solved several large-scale problems. Maiti and Sen [1998] modeled a solitary wave propagation and run-up on slope by using a higher-order BIEM where a cubic-spline variation of the geometry and boundary variables was assumed to ensure the higher-order smoothness of the solution.

Zhou and Stansby [1998] extended an Arbitrary Lagrangian-Eulerian model in the σ coordinate system (ALE σ) for shallow water flows, based on the unsteady Reynolds-averaged Navier-Stokes equations. The standard $k - \epsilon$ turbulence model was used to calculate the

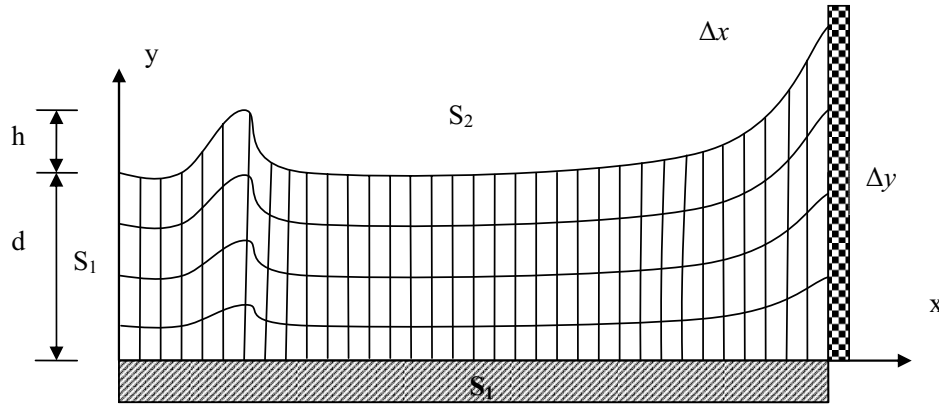


Figure 1 : A definition sketch for a progressive wave in the physical domain.

eddy viscosity time.

L. Gaston and A. Camara [2000] presented a two-dimensional Lagrangian-Eulerian finite element approach for non-steady state turbulent fluid flows with free surfaces. Their model was based on a velocity-pressure finite element Navier-Stokes solver, including an augmented Lagrangian technique and an iterative resolution of Uzawa type. Turbulent effects were taken into account with the $k - \epsilon$ two-equation statistical model. Mesh was updated using an arbitrary Lagrangian-Eulerian (ALE) method for a proper description of the free surface evolution. Loa and Shaob [2002] developed an incompressible Smoothed Particle Hydrodynamics (SPH) method with a Large Eddy Simulation (LES) approach to simulate the near-shore solitary wave mechanics. They solved the incompressible Navier-Stokes equations in Lagrangian form using a two step fractional method for a solitary wave against a vertical wall and its run-up.

3 Governing Differential Equations Based on Full ALE Approach

The surface motion and run-up for unsteady motion of a surface wave under gravity is evaluated by solving the governing equations using a Full Arbitrary Eulerian-Lagrangian method. By introducing the following variables:

$$\begin{aligned} \bar{x} &= x\bar{d}, & \bar{y} &= y\bar{d}, & \bar{p} &= p\bar{\rho}\bar{g}\bar{d}, & \bar{u} &= u(\bar{g}\bar{d})^{1/2} \\ \bar{v} &= v(\bar{g}\bar{d})^{1/2}, & \bar{t} &= t\left(\frac{\bar{d}}{\bar{g}}\right)^{1/2} \end{aligned} \quad (1)$$

The dimensionless form of the governing equations in the

Arbitrary Lagrangian-Eulerian description is:

$$\begin{aligned} \frac{\partial u}{\partial t} \Big|_{\xi, \eta} + (u - w_u) \frac{\partial u}{\partial x} + (v - w_v) \frac{\partial u}{\partial y} \\ = -\frac{\partial p}{\partial x} + \frac{1}{Re} \left(\frac{\partial^2 u}{\partial x^2} + \frac{\partial^2 u}{\partial y^2} + \frac{\partial}{\partial x} \left(\frac{\partial u}{\partial x} + \frac{\partial v}{\partial y} \right) \right) \end{aligned} \quad (2)$$

$$\begin{aligned} \frac{\partial v}{\partial t} \Big|_{\xi, \eta} + (u - w_u) \frac{\partial v}{\partial x} + (v - w_v) \frac{\partial v}{\partial y} \\ = -\frac{\partial p}{\partial y} + \frac{1}{Re} \left(\frac{\partial^2 v}{\partial x^2} + \frac{\partial^2 v}{\partial y^2} + \frac{\partial}{\partial y} \left(\frac{\partial u}{\partial x} + \frac{\partial v}{\partial y} \right) \right) - 1 \end{aligned} \quad (3)$$

$$\frac{\partial u}{\partial x} + \frac{\partial v}{\partial y} = 0 \quad (4)$$

$$\frac{\partial h}{\partial t} \Big|_{\xi, \eta} + (u - w_u) \frac{\partial h}{\partial x} - v = 0 \quad (5)$$

where \bar{x} (x) and \bar{y} (y) are physical coordinate system, ξ and η are reference coordinate system, \bar{u} (u) and \bar{v} (v) are particle velocities in x and y directions, w_u and w_v are mesh velocities in x and y directions, \bar{p} (p) is pressure, \bar{h} (h) is position of the free surface relative to bed, \bar{t} (t) is time, \bar{d} (d) is undisturbed water depth, g is gravity acceleration, Re is Reynolds number and ρ is fluid mass density. All the parameters in parentheses show the dimensionless value of their equivalent parameter.

The boundary conditions for the Arbitrary Lagrangian-Eulerian formulation are identical to those for the Eulerian or Lagrangian methods. The boundary consists of two types: the boundary on which velocity is given like run-up wall and bed, and the free surface boundary on

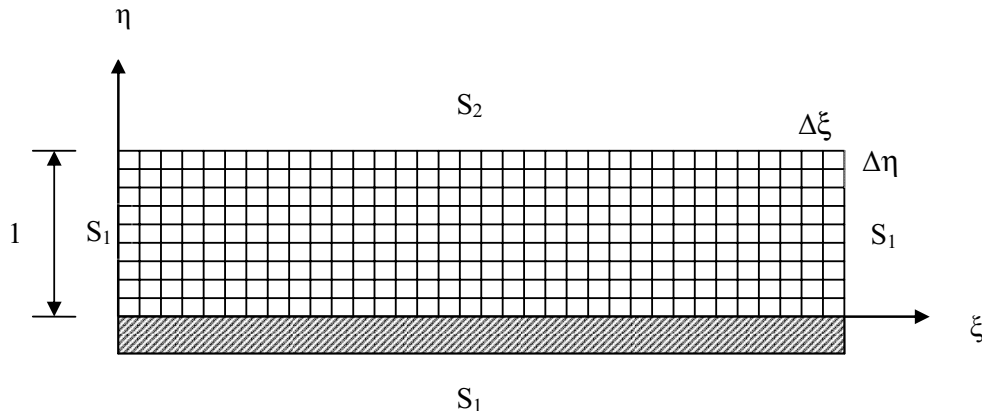


Figure 2 : A definition sketch showing computational domain

which the surface force is specified as traction force. The second boundary appears as natural boundary conditions in the discretised equations. The boundary conditions associated with Equations 2 to 5 can be expressed as:

$$u = \hat{u} \quad \text{on} \quad \bar{s}_1 \tag{6}$$

$$v = \hat{v} \quad \text{on} \quad \bar{s}_1 \tag{7}$$

$$\left(-p + \frac{2}{Re} \frac{\partial u}{\partial x}\right) \cdot n_x + \frac{1}{Re} \left(\frac{\partial u}{\partial y} + \frac{\partial v}{\partial x}\right) \cdot n_y = \hat{c}_x \quad \text{on} \quad \bar{s}_2 \tag{8}$$

$$\frac{1}{Re} \left(\frac{\partial u}{\partial y} + \frac{\partial v}{\partial x}\right) \cdot n_x + \left(-p + \frac{2}{Re} \frac{\partial v}{\partial y}\right) \cdot n_y = \hat{c}_y \quad \text{on} \quad \bar{s}_2 \tag{9}$$

Where the superscript caret (^) denotes a function which is given on the boundary and n_x, n_y show the direction cosines of the outward normal to the boundary with respect to coordinates x and y .

4 Transformation Into Computational Domain.

The weak formulation of equations 2 to 5 is obtained by multiplying the differential equations by suitable functions and integrating over a domain V , which is bounded by a surface S with a unit normal vectors in x and y directions n_x, n_y .

Computing the propagation of free surface waves involves computational boundaries that do not coincide with coordinate lines in physical space. This requires a complicated interpolation function (shape function) on the local grid lines. Transformation of the wave propagation model from the physical domain, (x, y, t) to a computational domain, (ξ, η, t) simplifies the problem of highly deformed air / fluid interface that arises in the

analysis of wave propagation. The distorted region in physical space is mapped into a rectangular region in the generalized coordinate space, where the unknown interface coincides with a coordinate line as shown in Fig. 2.

To perform finite element discretization, the variational equations in the global physical coordinates is written in terms of the generalized coordinates (ξ, η) . This requires the coordinate transformation of derivatives. Using the relationships between the physical (x, y) and Computational (ξ, η) coordinates, the variational equations and the boundary conditions can be written in terms of the generalized coordinates as independent variables and discretization is performed in the generalized coordinate system.

For grid generation, considering proper correspondence between points (x, y) in the irregular physical domain and points (ξ, η) in the regular computational domain, the following mapping can be established:

$$x = \sum_{i=1}^3 (\xi + h\alpha_i) F_i(\eta) \tag{10}$$

$$y = \eta(1 + h) \tag{11}$$

Where α_i are parameters used in mapping and the function $F_i(\eta)$ is three-point interpolation function defined as:

$$\begin{aligned} F_1(\eta) &= 1 - 3\eta + 2\eta^2 \\ F_2(\eta) &= 4\eta - 4\eta^2 \\ F_3(\eta) &= -\eta + 2\eta^2 \end{aligned} \tag{12}$$

The three parameters $\alpha_i, (i=1,2,3)$ should be specified, in further steps. Detection of the instances where the

wave profile is not uniquely defined requires evaluation of the Jacobian of the transformation matrix. For a single value mapping, the Jacobian of the transformation matrix should be finite and nonzero. This transformation is used in the modeling of wave propagation and run-up both over sloping beaches, where the evolution occurs over bathymetry topography, and over constant depth regions.

4.1 Spatial Transformation Relationship

Since the transformation functions defined in Equations 10 and 11 must be capable of mapping a variety of wave forms, a general mapping valid for all cases is not easy to define. For example, in non breaking waves, α_i can be equal to zero. On the other hand α_i play a significant role in mapping breaking waves and also large surface deformations. Several specific transformational functions are as follows.

4.1.1 Eulerian description

To have an Eulerian description, where the physical coordinate system coincide with the generalized coordinate system, it is necessary to set $\alpha_1 = \alpha_2 = \alpha_3 = 0$.

4.1.2 Eulerian description in x direction and Lagrangian description in y direction

Eulerian Description in x direction and Lagrangian Description in y direction can be applied for non-breaking waves. In this case, it is necessary to set $\alpha_1 = \alpha_2 = \alpha_3 = 0$. The transformation is Lagrangian in y direction and Eulerian in x direction and the problems associated with this transformation should have single value profile. By the way, this transformation can be used for spill breaking waves where breaking does not happen in the same way as in the plunging breaking case.

4.1.3 Arbitrary Lagrangian-Eulerian Description

The Arbitrary Lagrangian-Eulerian algorithm is employed in modeling wave propagation both over sloping beaches, where the evolution occurs over bathymetry topography, and over constant depth regions. Although this transformation is convenient for breaking waves, non-breaking waves can also be treated using the same mapping. In Fig. 3 different types of α_3 values are provided and depending on the nature of the problem, some particular relationships between the undefined parameters α_1 ,

α_2 and α_3 and the defined parameters ξ , t and h can be obtained.

As shown in Fig. 3, three different categories can be considered as follows:

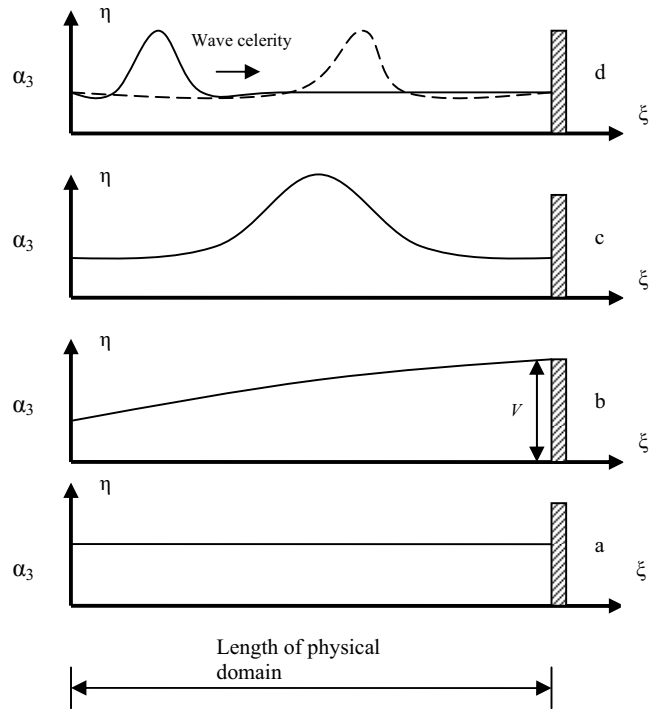


Figure 3 : Different type of α_3 function

- A. All of the α_i values are considered to be constant (a).
- B. The α_i values are considered to be only a function of ξ as (b and c).
- C. The α_i values are functions of ξ and t or their values depend on h as (d).

Based on the nature and boundary conditions of the problem, one of the above three cases can be deployed.

4.2 Variational Equations in the Transformed Domain

Spatial discretization of partial differential equations in the numerical model is based on a Galerkin finite element method. This method is implemented using the weighted residual variational method for solution within each element. Using standard linear shape functions for a rectangular element in natural coordinate system, the velocity, pressure and correction potential fields within the

element are interpolated in terms of their nodal values as follows:

$$\begin{aligned} u_i &= \Psi_j u_{ij}, \quad j = 1, 4, \quad [i = 1, 2] \\ p &= \Psi_j p_j, \quad j = 1, 4 \\ \phi &= \Psi_j \phi_j, \quad j = 1, 4 \\ h &= \Psi_j h_j, \quad j = 1, 2 \end{aligned} \quad (13)$$

Where Ψ_j is the interpolation function and u_{ij}, ϕ_j, p_j and h_j represent the nodal values at the j^{th} node of the element. ϕ is a scalar which is referred to as the correction potential base on the Fractional step method presented by Hayashi and hatanaka (1991). By dividing the total time t into a number of short time increments Δt , the equations of motion, continuity and kinematic boundary condition, (Equations 2 to 5), can be discretized into:

$$\begin{aligned} M_{ab} |J^{-1}|^{n+1} \tilde{u}_{ib}^{n+1} &= M_{ab} |J^{-1}|^n \tilde{u}_{ib}^n \\ &- \frac{\Delta t}{Re} \left[\left(\frac{2}{j} \delta_{i,1} + j \delta_{i,2} \right) \xi_{k,j}^n \xi_{l,j}^n M_{akbl} \right] |J^{-1}|^n u_{ib}^n \\ &- \frac{\Delta t}{Re} \xi_{l,1}^n \xi_{j,2}^n (\delta_{il} M_{ajbl} u_{2b}^n + \delta_{i2} M_{albj} u_{1b}^n) |J^{-1}|^n \\ &- \Delta t \left[\xi_{l,j}^n M_{abbl} (u_{jb}^n - w_{u,jb}^n) \right] |J^{-1}|^n u_{ib}^n \\ &+ \Delta t \xi_{j,i}^n M_{ajb} |J^{-1}|^n p_b^n + \sum_{\xi_i}^n, \end{aligned} \quad (14)$$

where

$$\begin{aligned} \sum_{\xi_i}^n &= \left(-p_b^n H_{ab} + \frac{2}{Re} \xi_{j,i}^n H_{abj} u_{ib}^n \right) \\ &[(x_{2,2}^n n_{\xi_1} - x_{2,1}^n n_{\xi_2}) \delta_{i,1} + (x_{1,2}^n n_{\xi_1} - x_{1,1}^n n_{\xi_2}) \delta_{i,2}] \\ &+ \frac{1}{Re} (\xi_{j,2}^n H_{abj} u_{1,b}^n + \xi_{j,1}^n H_{abj} u_{2b}^n) \\ &[(x_{2,2}^n n_{\xi_1} - x_{2,1}^n n_{\xi_2}) \delta_{i,2} + (x_{1,2}^n n_{\xi_1} - x_{1,1}^n n_{\xi_2}) \delta_{i,1}] \end{aligned}$$

$$\begin{aligned} &(\xi_{l,j}^{n+1})^2 M_{albl} + \xi_{l,j}^{n+1} \xi_{2,l}^{n+1} (M_{al2} + M_{a2l}) |J^{-1}|^{n+1} \phi_b \\ &= \xi_{j,l}^{n+1} M_{abj} |J^{-1}|^{n+1} \tilde{u}_{lb}^{n+1} + \Phi_s^{n+1} \end{aligned} \quad (15)$$

where

$$\Phi_s^{n+1} = \xi_{j,i}^n H_{abj} \phi_b^{n+1} [(x_{2,2}^{n+1} n_{\xi_1} - x_{2,1}^{n+1} n_{\xi_2}) \delta_{l,k}]$$

$$+ (x_{1,2}^{n+1} n_{\xi_1} - x_{1,1}^{n+1} n_{\xi_2}) \delta_{2,k}]$$

$$M_{ab} u_{ib}^{n+1} = M_{ab} \tilde{u}_{ib}^{n+1} + \xi_{j,i}^{n+1} M_{abj} \phi_b \quad (16)$$

$$M_{ab} |J^{-1}|^{n+1} p_b^{n+1} = M_{ab} |J^{-1}|^n p_b^n - \frac{1}{\Delta t} M_{ab} |J^{-1}|^{n+1} \phi_b \quad (17)$$

$$\begin{aligned} H_{ab} |J^{-1}|^{n+1} h_b^{n+1} &= H_{ab} |J^{-1}|^n h_b^n + \Delta t (H_{ab} |J^{-1}|^{n+1} u_{2b} \\ &- \xi_{j,1}^n H_{abj} (u_{1b}^{n+1} - w_{u,1b}^{n+1}) |J^{-1}|^{n+1} h_b^n \end{aligned} \quad (18)$$

Note that due to the complexity, the equations are written in the mapped domain, using indicial notation. Change of the indices is as:

$$\{i = 1, 2 \quad [k = 1, 2 \quad (l = 1, 2 \quad "j = 1, 2")]\}.$$

Here, $\sum_{\xi_i}^n$ and Φ_s^{n+1} are boundary integrals, created in the weak formulations of governing equations, ξ_i is the reference coordinate system ($\xi_1 = \xi$ and $\xi_2 = \eta$ direction), $|J^{-1}|$ is the Jacobian inverse of transformation matrix and the following definitions are for the consistent mass matrix obtained from analytical integration used to write the above equations.

$$\begin{aligned} M_a &= \int_V \Psi_l dv, \quad M_{ab} = \int_V \Psi_a \Psi_b dv, \\ M_{aJb} &= \int_V \Psi_{a,J} \Psi_{b,j} dv, \quad M_{ajb} = \int_V \Psi_{a,j} \Psi_b dv, \\ M_{abj} &= \int_V \Psi_a \Psi_{b,j} dv \end{aligned} \quad (19)$$

$$M_{abbj} = \int_V \Psi_a \Psi_b \Psi_{b,j} dv, \quad H_{ab} = \int_V \Psi_a \Psi_b ds,$$

$$H_{abj} = \int_V \Psi_a \Psi_{b,j} ds, \quad H_{abbj} = \int_V \Psi_a \Psi_b \Psi_{b,j} ds,$$

It should be noted that all of the derivations are with respect to ξ_i .

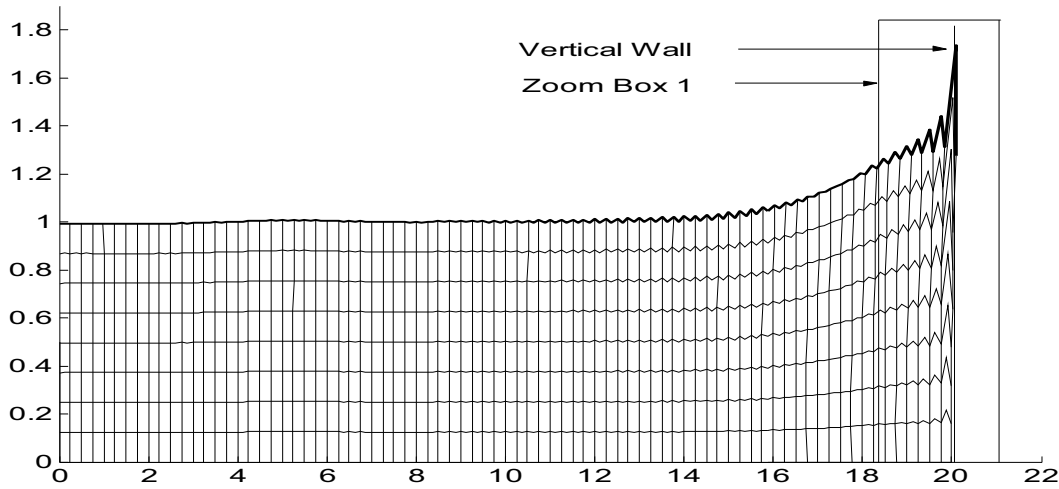


Figure 4 : Oscillations at the vertical wall in physical domain.

4.3 Deficiency on the boundary

In the full Arbitrary Lagrangian-Eulerian approach, nodal points move in both directions in physical domain, so there must be important notice on solid boundaries like vertical wall to avoid oscillations near the vertical boundary (Fig. 4). Dolatshahi and Wellford [1995] considered α_1 equal to zero and α_2 as:

$$\alpha_2 = \frac{\alpha_3 h}{2(1+h)} \quad (20)$$

Hence for predicting wave run up over vertical wall, they assumed α_3 equal to zero and employed fix Eulerian description in wave propagation direction and Lagrangian computation for free surface line in vertical direction.

In their approach, since there was no mesh movement in the x direction, the right side boundary in computational domain coincided with the vertical wall in physical domain without any oscillations.

The deficiency in their method was free surface oscillations at the boundaries with a non-zero α_3 (Fig. 4).

These oscillations are due to improper mapping on the vertical wall. Considering Equation 10 and the value of $F_1(\eta) = F_2(\eta)=0$ and $F_3(\eta)=1$ on the surface, the physical displacement in x direction on the surface at the wall point is computed as:

$$x(wall) = \xi(wall) + \alpha_3.h \quad (21)$$

The physical domain is mapped into a rectangular domain, whereas the last physical node, "x (wall)", that is

related to the last computational node ξ (wall), will be out of physical domain and the value of offset is equal to $(\alpha_3.h)$, as illustrated in Fig. 5. To control oscillations, a moving boundary technique is introduced.

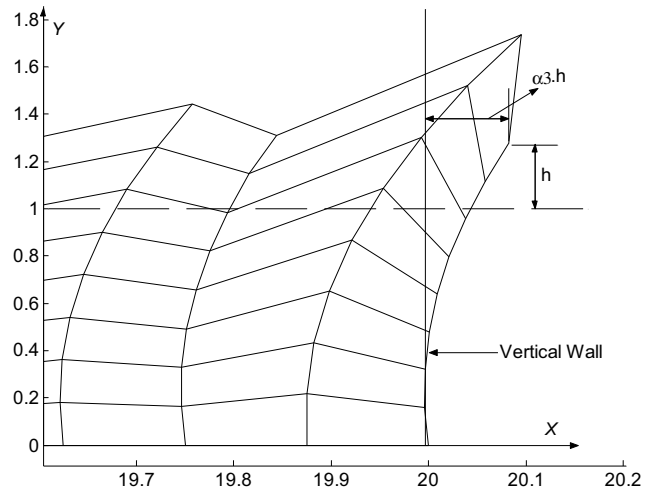


Figure 5 : Boundary offset (Zoom Box 1)

4.4 Moving Boundary and Numerical Techniques

Two approaches are considered to address the aforesaid deficiency on the boundary. In the first approach, an efficient equation is introduced for α_3 on the surface which is zero on the boundary to control oscillation. In the second approach, the nodal movements at the bottom are equal

to the nodal movements on the surface, and by using a moving boundary technique; the nodes in the physical domain coincide with the nodes in computational domain at the wall point.

4.4.1 Fifth order polynomial technique

Oscillations at the boundary can be controlled by eliminating the physical node offset at the boundary as is illustrated in Fig. 5. Except the bottom node at the boundary, all the nodal points move out of the physical domain. The reason for this movement is due to Full Arbitrary Lagrangian-Eulerian approach that creates an offset equal to:

$$offset = \sum_{i=1}^3 (h\alpha_i) F_i(\eta) \tag{22}$$

To coincide physical and computational boundary at the wall, a fifth order polynomial function is used for α_3 to delete offsetes on the boundary. The values of α_i and their derivatives are considered zero at the intersection of common blocks. This assumption makes it possible to have different definitions for α_i at different segments and keep the values of α_2 and α_3 equal to zero at certain arbitrary points such as boundary points.

$$\alpha_3 = \frac{b}{\varepsilon^3 l^5 (1-\varepsilon)^3} [2(\xi - \xi_0)^5 (2\varepsilon - 1) + l(\xi - \xi_0)^4 (4 - 5\varepsilon - 5\varepsilon^2) + 2l^2(\xi - \xi_0)^3 (-1 - \varepsilon + 5\varepsilon^2) + l^3 \varepsilon \beta (\xi - \xi_0)^2 (3 - 5\varepsilon)] \tag{23}$$

$$\alpha_2 = c\alpha_3 \quad 0 < C < 0.5 \tag{24}$$

Definitions of b , ε , l and ξ_0 are illustrated in Fig. 6 Parameter C is a constant coefficient and it's value is obtained by trial and error to stabilize the problem.

One of the great advantages of this approach is to control mesh movement by changing the value of coefficient b as illustrated in Fig. 6. For different value of coefficient b and fix number of elements, the results of run-up for a solitary wave with a normalized amplitude $H=0.2$, when the wave climbs up to the maximum height, are presented in Tab 1.

Respectively, Tab. 1 shows the results of run-up for a range of values for α_3 from zero to 4. Comparing the result with the exact analytical solution presented by Laiton

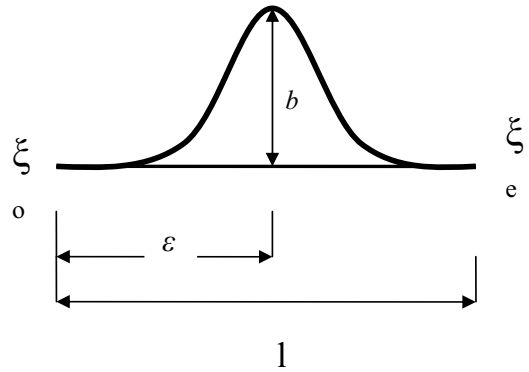


Figure 6 : definition of parameters in α_3 function.

Table 1 : Comparison of the run-up for solitary wave with a normalized amplitude $H=0.2$ when the wave climbs up the right wall to the maximum height applying different b value.

| Normalized Amplitude $H=0.2$ grid 160×8 , $\Delta t = 0.25$ | |
|---|-----|
| Run-up | B |
| 1.42739 | 0 |
| 1.42352 | 0.1 |
| 1.42022 | 0.2 |
| 1.41722 | 0.3 |
| 1.41343 | 0.4 |
| 1.39608 | 1 |
| 1.36149 | 3 |
| 1.35015 | 4 |

[1960] where the height of run-up value is 0.4200, it can be observed the best result is obtained when α_3 is equal to the wave height. For better judgment about the efficiency and effectiveness of Full Arbitrary Lagrangian-Eulerian algorithm, the results of mesh refinement in Dolatshahi and Wellford [1995] algorithm which is Eulerian in x and Lagrangian in y direction are presented in Tab. 2.

Tab. 2 shows that mesh refinement does not lead to a better convergence to the exact analytical result presented by Laiton [1960]. In Tab. 3 results of analytical solution and Dolatshahi & Wellford approach are compared with the present algorithm.

Table 2 : Mesh refinement and comparison of the maximum run-up for a solitary wave with normalized amplitude of $H=0.2$.

| Mesh Refinement | | |
|------------------------|---------------------------|-----------------------|
| Grid Properties | | Maximum Run-Up |
| Grid Dimension | Number Of Elements | |
| 140*7 | 980 | 0.44800 |
| 160*8 | 1280 | 0.44780 |
| 180*9 | 1620 | 0.44800 |
| 200*10 | 2000 | 0.44780 |
| 220*11 | 2420 | 0.44799 |
| 240*12 | 2880 | 0.44796 |

4.4.2 Equal movement and moving boundary

One of the advantages of Full Arbitrary Lagrangian-Eulerian scheme is mesh movement in any direction which gives the ability of modeling high deformations. In this method, nodal points can move in both coordinate directions by introducing appropriate mapping functions as defined in equations 10 and 11. Oscillations at the boundary resulted from the offsets of physical nodal points at the boundary that do not coincide on the computational domain is shown in Fig. 5. Another approach to eliminate oscillations is to force equal movements for all of the nodes on the boundary. By using moving boundary technique, physical boundary will coincide with the computational boundary. In this approach assuming $\alpha_1 = \alpha_2 = \alpha_3 = v$, will make the nodal points on the boundary to move and create an offset equal to:

$$\text{Boundary offset} = v.h = \alpha_3.h \tag{25}$$

Where h is the run-up height and v is a constant coefficient, which controls the boundary offset. The value of v is proportional to wave height and obtained by trial and error to stabilize the problem (Fig.3-b).

To have a result close to the analytical solution for a solitary wave with wave height equal to 0.2, the optimum value of 0.018 for v is obtained by trial and error as in Tab. 4.

In moving boundary technique, the width of the elements at the boundary decreases gradually proportional to the boundary offset. So, at each time step, the mass matrix will change due to the changes in the dimensions of the element attached to the boundary. The offset increases in

each time step due to the height of run-up on the vertical wall. By introducing equation 10, $x(\text{wall})$ is computed as:

$$x(\text{wall}) = \xi(\text{wall}) - (\text{Boundary offset}) + \alpha_3.h = \xi(\text{wall})$$

Hence the physical boundary will coincide with computational boundary, and the oscillations are controlled. Results of these two techniques are compared with the previous results and the analytical solution in Tab. 5.

To assess the accuracy of the present approach, the maximum run-up of the solitary waves with different amplitudes is computed. Results are compared with the experiment, marker-and-cell (MAC) method done by Chan and Street [1970], analytical solution presented by Laiton [1960], the I-SPH computation done by Lo and Shao [2002],

Fourier analysis done by Fenton [1982] and finally results by Maiti and sen [1999].

For $H/d = 0.1$ to 0.3 results obtained by the present method show a good agreement with experimental and analytical results. It is also in good agreement with results by Maiti [1999] for all the wave height ranges. This agreement could be due to using Navier Stokes equations and full nonlinear free surface boundary in both approaches, while for H/d above 0.3 , the present results are slightly smaller in magnitude than experimental data and Fenton [1982] who used the Fourier method. Analytical solution by Laiton's [1960] underestimates experimental results when H/d is greater than 0.4 . This difference results from the nonlinearity effect which is ignored in the analytical solution. For H/d greater than 0.4 , the I-SPH method used by Lo and Shao [2002] overestimates the experimental results.

5 Conclusion

The Full Arbitrary Lagrangian Eulerian method with a mapping technique was developed to solve free surface wave propagation and run-up over vertical wall. One of the advantages of this method is controlling the mesh movement in any direction which makes it possible to model high deformations. Calculating the exact analytical result for wave run-up is also possible in this method by changing a controlling coefficient to find the best transformation shape with the selected mapping functions. This coefficient gives the calibration capability to the model for a wide range of free surface problems. No smoothing or artificial viscosity is needed to control os-

Table 3 : Comparing the results of present algorithm with previous works.

| Comparing Approaches | | | | |
|---|-----------|-----------|--------------------|----------------|
| Algorithm | Time Step | Iteration | Number Of Elements | Maximum Run Up |
| Eulerian in x & Lagrangian in y direction(Dolatshahi & Wellford[1995]) | 0.025 | 388 | 1280 (160 * 8) | 0.44780 |
| Full arbitrary Lagrangian_Eulerian in both direction with fifth order polynomial (present approach) | 0.025 | 386 | 1280 (160 * 8) | 0.42022 |
| Analytical solution(Laiton [1960]) | | ----- | ----- | 0.42000 |

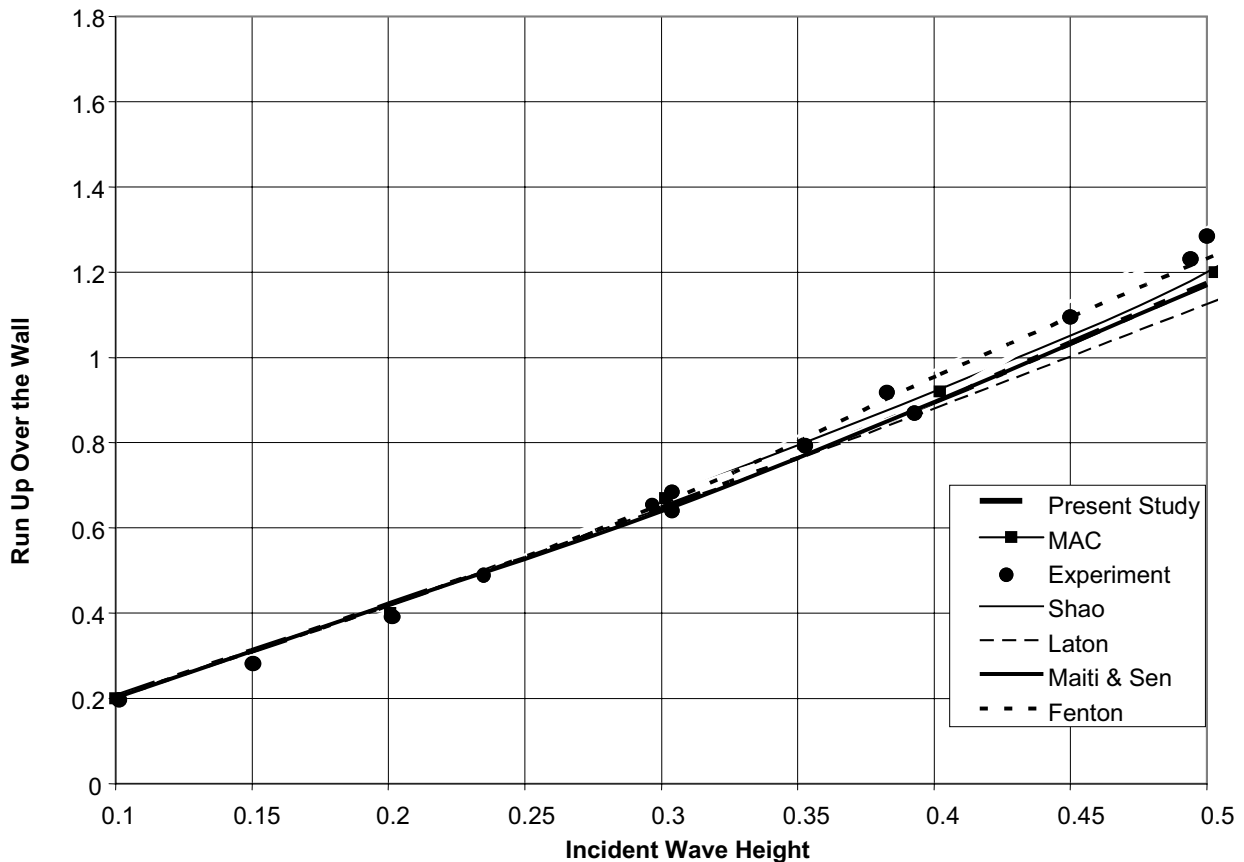


Figure 7 : Comparison of the run-up for a solitary wave with different normalized amplitudes at the time when the wave climbs on the right wall up to the maximum height by different approaches.

cillations of run-up on boundary which are eliminated by a moving boundary and fifth order mapping.

In a previous Arbitrary Lagrangian-Eulerian method presented by Dolatshahi and Wellford [1995], there was no convergence to exact analytical result but in the Full Arbitrary Lagrangian-Eulerian model, convergence is satisfactory. The model is validated against the analytical and experimental results. The model can be employed in

Table 4 : Comparison of the run-up for a solitary wave on the right wall with a normalized amplitude $H=0.2$ applying different value for v .

| V | Maximum Run-Up |
|-------|----------------|
| 0.01 | 0.4281 |
| 0.017 | 0.4218 |
| 0.018 | 0.4203 |
| 0.02 | 0.4163 |

Table 5 : Comparison of the run-up for a solitary wave with a normalized amplitude $H=0.2$ at the time when the wave climbs on the right wall up to the maximum height.

| Normalized amplitude $H=0.2$ | | | | |
|-------------------------------------|--------------------|-----|-----------|--------|
| Algorithm | Number of elements | L | Time step | Run-up |
| Dolatshahi | 1280 | 20 | 0.025 | 0.4478 |
| Hayashi | 2048 | 16 | 0.01 | 0.4486 |
| Ramaswamy | 2048 | 16 | 0.02 | 0.4480 |
| Grilli | ---- | 20 | ---- | 0.4250 |
| Fifth order polynomial technique | 1280 | 20 | 0.025 | 0.4202 |
| Equal movement with moving boundary | 1280 | 20 | 0.025 | 0.4203 |
| Analytical solution (Laton) | ---- | --- | ---- | 0.4200 |

any geometry, under complicated boundary conditions, and with arbitrary bathymetry, without any additional computational effort. The method is tested on a free unsteady wave of finite amplitude and is found to give excellent agreement with independent calculations based on the other existing theories. Finally, it is recommended to solve free surface problems with new techniques like mesh less methods and considering turbulent effects with $k-\epsilon$ equations to compare the results with other previous results.

References

Atluri, S. N; Han, Z. D.; Rajendran A. M. (2004): A New Implementation of the Mesh less Finite Volume Method. Through the MLPG “Mixed” Approach, *CMES: Computer Modeling in Engineering & Sciences*, Vol. 6, No. 6, pp. 491-514

Atluri, S.N. (2004): The Meshless Method (MLPG) for Domain & BIE Discretizations. 700 pages, Tech Science Press.

Camfield, F. E. ; Street, R.L. (1969): Shoaling of Solitary Waves on Small Slopes. Department of Civil Engineering, Stanford University, California.

Camfield, F. E. ; Street, Robert L. (1967): An Investigation of the Deformation and Breaking of Solitary Waves. Technical Report No. 87, Department of Civil Engineering, Stanford University, California.

Chan, K.C. ; Street, R. L. (1970): A computer study of finite amplitude water wave. *J Comput Phys*, 6:68–94.

Dolatshahi, P. M. ; Wellford, C. L. (1995): Finite element methods for viscous free surface fluids including

breaking and non-breaking waves. PhD Thesis, University of Southern California, California.

Fenton, J.D. ; Rienecker, M.M. (1982): A Fourier method for solving nonlinear water-wave problems, application to solitary-wave interactions. *Journal of Fluid Mechanics*, 118, 411–443.

Gaston, L.; Kamara, A. (2000): Arbitrary Lagrangian-Eulerian finite element approach to non-steady state turbulent fluid flow with application to mould filling in casting. *International Journal for Numerical Methods in Fluids*, v 34, n 4, p 341-369 .

Grilli, S. T.; Svendsen, I. A. (1989): Computation of nonlinear wave kinematics during propagation and runup on a slope. NATO Workshop, Molde, Norway.

Grilli, S. T.; Svendsen, I. A.; Subramanya, R. (1997): Breaking criterion and characteristics for solitary waves on slopes. *Journal of Waterway, Port, Coastal, and Ocean Engineering*, ASCE 123 (3), 102–112.

Hayashi, M.; Hatanaka, K.; Kawahara, M. (1991): Lagrangian Finite Element Method for Free Surface Navier-Stokes Flow Using Fractional Step Methods. *International Journal for Numerical Methods in Fluids*, Vol. 13, 805-840.

Heitner, K. L. (1969): A Mathematical Model for calculation of the Run-up of Tsunamis. PhD. thesis, California Institute of Technology, Pasadena, California.

Ippen, A. T.; Mitchell, M. M. (1957): The Damping of the Solitary Wave from Boundary Shear Measurements. Hydrodynamics Laboratory, M.I.T., Technical Report No. 23.

Keulegan, G. H. (1948): Gradual Damping of Solitary

- Waves. *Journal of Research of the National Bureau of Standards*, Vol. 40, Research Paper.
- Kim, S. K.; Liu, P. L. F.; Liggett, J. A.** (1983): Boundary Integral Equation Solutions for Solitary Wave Generation, Propagation and Run-Up. *Coastal Engineering*, 7, 299-317.
- Laiton, E. V.** (1960): The Second Approximation to Cnoidal and Solitary Waves. *Journal of Fluid Mechanics*, Vol. 9, Part 3, pp 430-444.
- Lin P. Z.; Chang K. A.; Liu Philip L. F.** (1999): Run-up and run-down of solitary waves on sloping beaches. *J Waterway Port, Coast Ocean Engng*, ASCE, 125(5), 247-55.
- Lo, E. Y. M.; Shao, S.** (2002): Simulation of near-shore solitary wave mechanics by an incompressible SPH method. *Applied Ocean Research*, Volume 24, Issue 5, Pages 275-286.
- Ma, Q. W.** (2004): Meshless Local Petrov Galerkin Method for Two Dimensional Water Wave Problems. *Journal of Computational Physics*, (In press).
- Maiti S.; Sen, D.** (1999): Computation of solitary waves during propagation and runup on a slope. *Ocean Engineering*, 26, 1063-1083.
- Ramaswamy, B.; Kawahara, M.** (1987): Arbitrary Lagrangian-Eulerian Finite Element Method for Unsteady, Convective, Incompressible Viscous Free Surface Fluid Flow. *International Journal for Numerical Methods in Fluids*, Vol. 7, 1053-1075.
- Synolakis, C. E.** (1987): The runup of solitary waves. *Journal of Fluid Mechanics*, 185, 523-545.
- Titov, V. V.; Synolakis, C. E.** (1995): Modeling of breaking and nonbreaking long-wave evolution and runup using VTCS-2. *J. Wtrwy. Port, Coast., and Oc. Engrg.*, ASCE, 121(6), 308-316.
- Vinje, T.; Brevig, P.** (1981): Numerical Simulation of Breaking Waves. *Adv. Water Resources*, Vol. 4.
- Wellford, C. L. Jr.; Ganaba, T. H.** (1981): A Finite Element Method with a Hybrid Lagrangian Line for Fluid Mechanics Problems Involving Large Free Surface Motion. *International Journal for Numerical Methods in Engineering*, 17, pp. 1201-1231.
- Zelt, J. A.** (1986): The Response of Harbors with Sloping Boundaries to Long Wave Excitation. Rep. KH-R-47, W., M. Keck Laboratory of Hydraulics and Water Resources, California Institute of Technology, Pasadena, CA. 318 pp.
- Zelt, J. A.** (1991): The Run-up of Non-Breaking and Breaking Solitary Waves. *Coastal Engineering*, 15, 205-246.
- Zhou, J. G. ; Stansby, P. K.** (1998): An arbitrary Lagrangian-Eulerian (ALE) model with non-hydrostatic pressure for shallow water flows. *Computer Methods in Applied Mechanics and Engineering*, Volume 178, Issues 1-2, Pages 199-214 .